Colloids and Surfaces A: Physicochem. Eng. Aspects 339 (2009) 13–19

Contents lists available at ScienceDirect

Colloids and Surfaces A: Physicochemical and Engineering Aspects

journal homepage: www.elsevier.com/locate/colsurfa

Engineering colloidal photonic crystals with magnetic functionalities

Wim Libaers[a], Branko Kolaric[a,b], Renaud A.L. Vallée[a,c], John E. Wong[d], Jelle Wouters[a], Ventsislav K. Valev[a], Thierry Verbiest[a], Koen Clays[a,*]

[a] Department of Chemistry, K.U. Leuven and Institute of Nanoscale Physics and Chemistry (INPAC), Celestijnenlaan 200D, 3001 Heverlee, Belgium
[b] Laboratoire Interfaces & Fluides Complexes, Centre d'Innovation et de Recherche en Matériaux Polymères, Université de Mons Hainaut, 20 Place du Parc, B-7000 Mons, Belgium
[c] Centre de Recherche Paul Pascal (CNRS), 115 avenue du docteur Schweitzer, 33600 Pessac, France
[d] RWTH Aachen University, Institute of Physical Chemistry, Landoltweg 2, 52056 Aachen, Germany

ARTICLE INFO

Article history:
Received 16 May 2008
Received in revised form 9 January 2009
Accepted 15 January 2009
Available online 23 January 2009

Keywords:
Photonic crystals
Magnetic colloids
Faraday rotation
Maghemite
Superparamagnetic

ABSTRACT

An engineering approach towards combined photonic band gap properties and magnetic functionalities, based on independent nanoscale engineering of two different materials at different length scales, is conceptually presented, backed by simulations, and experimentally confirmed. Large (>200 nm) monodisperse nanospheres of transparent silica self-assemble into a photonic crystal with a visible band gap, which is retained upon infiltration of small (<20 nm) nanoparticles of magnetic iron oxide. Enhancing and tuning Faraday rotation in photonic crystals is demonstrated.

1. Introduction

Magnetic nanoparticles are of great importance for various fields of chemistry and physics such as magnetic fluids and drug delivery, and magneto-optic data storage [1–8]. Considering their wide range of applications, various methods have been developed for their synthesis [1–4,9–11]. The size of these magnetic nanoparticles affects their properties. When the size of such a particle lies in the range of 5–25 nm, superparamagnetic behaviour is observed, i.e. every single nanoparticle becomes a single domain [1], behaves like a giant paramagnetic atom in a magnetic field and shows a fast response to magnetic fields with negligible remanence, which is essential for various applications [1]. In our research, we intend to use the superparamagnetic properties of iron oxide particles in order to design photonic crystals (PCs) with magnetic functionality.

PCs make up a new class of dielectric material in which the basic electromagnetic interaction is controllably altered over certain frequencies and length scales [12]. This control is achieved by creating spatially periodic dielectric structures in one (1D), two (2D) or three dimensions (3D). Due to the periodicity of the 3D dielectric medium, the propagation of light is inhibited in a given direction and for a given frequency range a photonic band gap is created. A convenient way to produce (3D) photonic crystals consists of ordering, through convective self-assembly [13,14], Langmuir–Blodgett deposition [15,16], sedimentation [17] or spin-coating [18,19] of monodisperse, colloidal spheres in colloidal crystals. In these colloidal crystals, the spectral position, width and amplitude of the band gap is a function of the size of the colloidal spheres and of the refractive index contrast between these spheres and the surrounding voids in the fcc, hcp or rhcp crystal structures obtained by close packing of the spheres. It should also be noted that the band gap in this type of photonic crystal is not a complete, omnidirectional band gap, but has some angular dependence, a property we exploit in this study.

The engineering of a photonic band gap material with magnetic functionality is one of biggest goals in the field of optical materials since magnetic materials can be used for additional control of the properties of light, e.g. nonreciprocal effects in the magnetic PCs [20,21]. Nonreciprocity, which is a known feature of magnetic photonic crystals [22], includes the possibility of unidirectional propagation of light. The use of magnetic particles with a high refractive index, like iron oxide particles, must also lead to an enhancement of the photonic band gap effect, in addition to the magnetic effects expected under application of an external magnetic field [23,24].

Considering our interest in using superparamagnetic particles for photonic applications, a size range of ~10 nm for the iron oxide particles is far too small to be used for fabrication of PCs with applications in the visible range. Additionally, at the bulk level, the magnetic particles are opaque, which is also not useful for photonic applications. In order to engineer crystals useful for photonic applications, we have considered several strategies that aim at increasing

* Corresponding author.
E-mail address: Koen.Clays@fys.kuleuven.be (K. Clays).

0927-7757/$ – see front matter © 2009 Elsevier B.V. All rights reserved.
doi:10.1016/j.colsurfa.2009.01.012

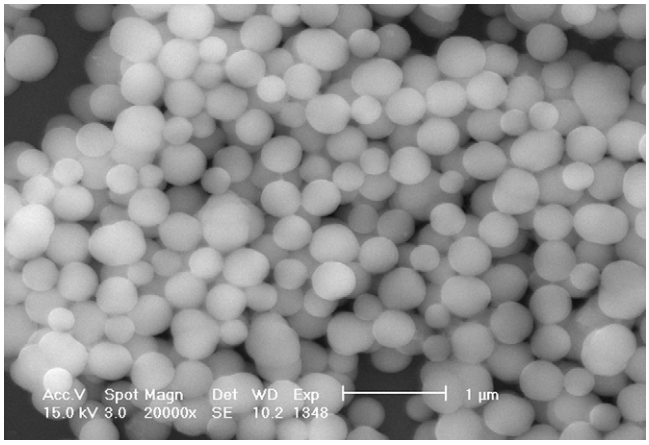

Fig. 1. SEM image of a layer of hybrid particles with an iron oxide core and a silica shell. Clearly, the polydispersity in size of the particles causes a lack of long-range ordering [22].

the size of the magnetic particles and making them transparent. A first attempt was made to create a magnetic photonic crystal in which superparamagnetic particles were used as a core for the synthesis of core–shell particles [25]. In this approach the superparamagnetic core was coated with silica using the classical Stöber method [26]. Note that the shell thickness then determines the total size of the particle. In that approach, the biggest problem was to control the size and monodispersity of the particles, and to suppress their intrinsic instability, which led to further polydispersity due to aggregation over long periods of time. The polydispersity of the core causes polydispersity of the hybrid particle making these hybrids inadequate for photonic applications [25]. The polydispersity of the core–shell particles was observed using SEM imaging (Fig. 1).

In this manuscript, two other approaches are explored to form PCs with magnetic properties. The motivation for our research was to establish a better protocol for designing core/shell photonic crystal as well as to see the effect of a high refractive index material on the photonic band gap. The first approach is to start by synthesizing monodisperse silica nanoparticles covalently functionalized with a coating of superparamagnetic particles on their surface, followed by the assembly of these colloidal particles, hopefully into a photonic crystal. The second approach, conversely, is to start by creating the photonic crystal from monodisperse silica nanospheres, which is only afterwards infiltrated with the superparamagnetic particles. Since iron oxide is incorporated into the silica photonic crystal (also known as an artificial opal), it is possible to at the same time investigate the effect of added high refractive index material on the band gap properties as well as the magnetic effect since the form of iron oxide used here has superparamagnetic properties. Comparative magnetic investigations were performed by measuring the Faraday rotation in a magnetic versus a non-magnetic photonic crystal, and in and out of the band gap.

2. Experimental part

2.1. Synthesis

Acid-stabilized maghemite colloids were prepared based on an existing procedure [9,10]. A solution of 16 mmol $FeCl_3$ and 8 mmol $FeSO_4$ in 200 ml of pure water was stirred at 500 rpm, and a 13.5 ml of 25% NH_3 aqueous solution was added rapidly to form black particles (magnetite), which were quickly precipitated using a permanent magnet. The supernatant was decanted, and the colloids were resuspended using 20 ml of 2 M nitric acid. Subsequently a solution of 10 mmol $Fe(NO_3)_3$ in 30 ml of water was added, and the suspension was stirred at 80 °C for 1 h to oxidize the particles to maghemite. The particles were then washed twice with 50 ml of 2 M nitric acid, and finally resuspended in 40 ml of water.

Silica colloids of approximately 200, 260 and 385 nm diameter were prepared using the Stöber method [26]. These were coated by functionalization with 3-mercaptopropyltrimethoxysilane (MPTMS) [9,10], by mixing 30 ml of a 1 mass% silica particle suspension in ethanol, with 0.5 ml MPTMS (85%) and 0.8 ml NH_3 25% in water. This mixture was stirred vigorously for 45 min, and then the temperature was raised to 76 °C to distill off about one-third of the ethanol. The remainder was then cooled and washed by centrifugation, the supernatant decanted, and the particles resuspended. This procedure was repeated twice with ethanol, then twice with water.

Coating the functionalized silica particles with the iron oxide particles was done by mixing equal volumes of the silica and maghemite suspensions obtained above and shaking strongly for 1 day. Excess iron particles were then removed by repeatedly allowing the silica to settle under gravitational forces and decanting the supernatant, which was then replaced with clean water. For the fabrication of PCs, the water was replaced by ethanol.

Convective self-assembly was used for the preparation of colloidal crystals from these suspensions [25,27]. This procedure is already well-established for unfunctionalized silica particles [13,28]. It is performed by putting a clean glass substrate vertically in a vial containing the ethanolic colloid suspension, and letting the solvent evaporate at a fixed temperature, typically at 33 °C in our experiments. The glass substrate and the vial containing the suspension were cleaned with piranha acid (2/3 sulfuric acid, 1/3 hydrogen peroxide as oxidant) prior to use.

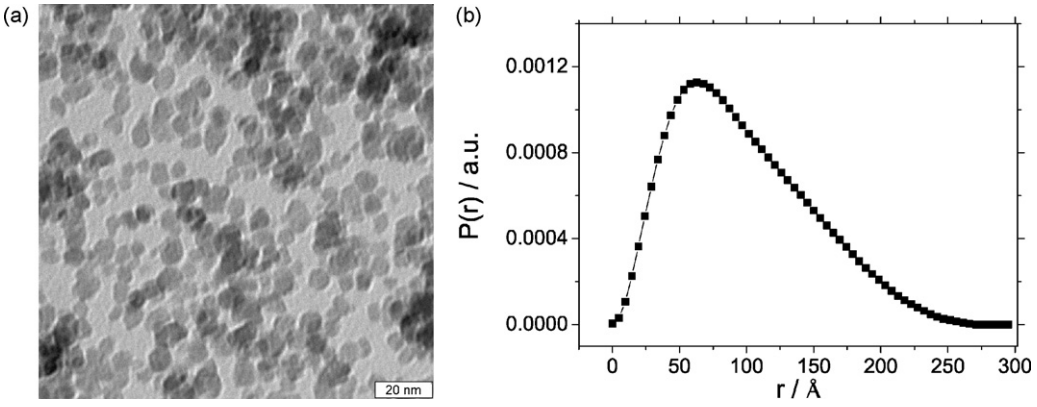

Fig. 2. (a) TEM image of iron oxide particles and (b) pair distance distribution function of the same iron oxide particles obtained by SAXS.

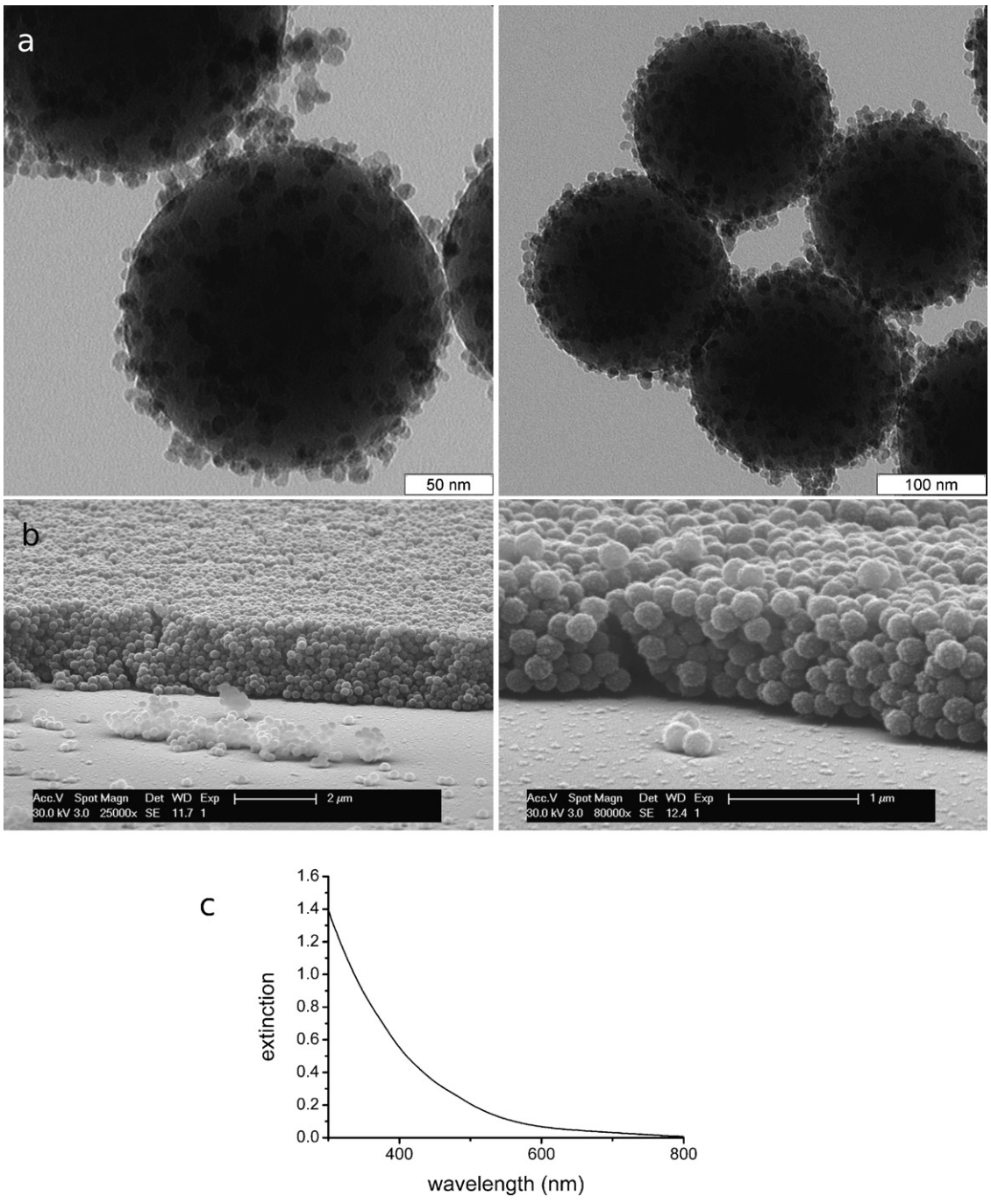

Fig. 3. (a) TEM images at several scales (indicated) of monodisperse spherical MPTMS functionalized silica particles coated by a layer of iron oxide particles. (b) SEM images from a multilayer film of the iron oxide-coated silica particles show a relatively dense packing. Nevertheless, the structures are less ordered than in typical PCs made of noncoated silica. (c) Transmission spectrum of such a multilayer film shows no evidence of a band gap.

3. Methods

Imaging of the particles was done using SEM (Philips Scanning Electron Microscope XL30 FEG). In order to make the surface conductive, a thin layer of gold was sputtered onto the sample.

Optical extinction spectra were performed on large areas (millimeter sized) to ascertain the quality and spectral features of the samples using a PerkinElmer Lambda 900 UV–VIS–NIR spectrophotometer. The vertical axis for these spectra uses a logarithmic scale, defined as follows: extinction = $-\log_{10}$(fraction of light transmitted).

Small angle X-ray scattering (SAXS) measurements were carried out on a S-Max3000 system with a MicroMaxTM-002 + X-ray microfocus generator (Rigaku). The Bayesian weighted distance distribution function p(r) was calculated from the angle dependent scattering using a fit routine included in the manufacturer supplied software [29].

TEM images were provided to us through a cooperation with the Max Planck Institute of Colloids and Interfaces (MPI KGF Golm, Germany).

Faraday rotation was measured at a wavelength of 830 nm on a homemade experimental setup [30,31].

Simulations were performed with the finite-difference time-domain (FDTD) method [32], using a freely available software package with subpixel smoothing for increased accuracy [33].

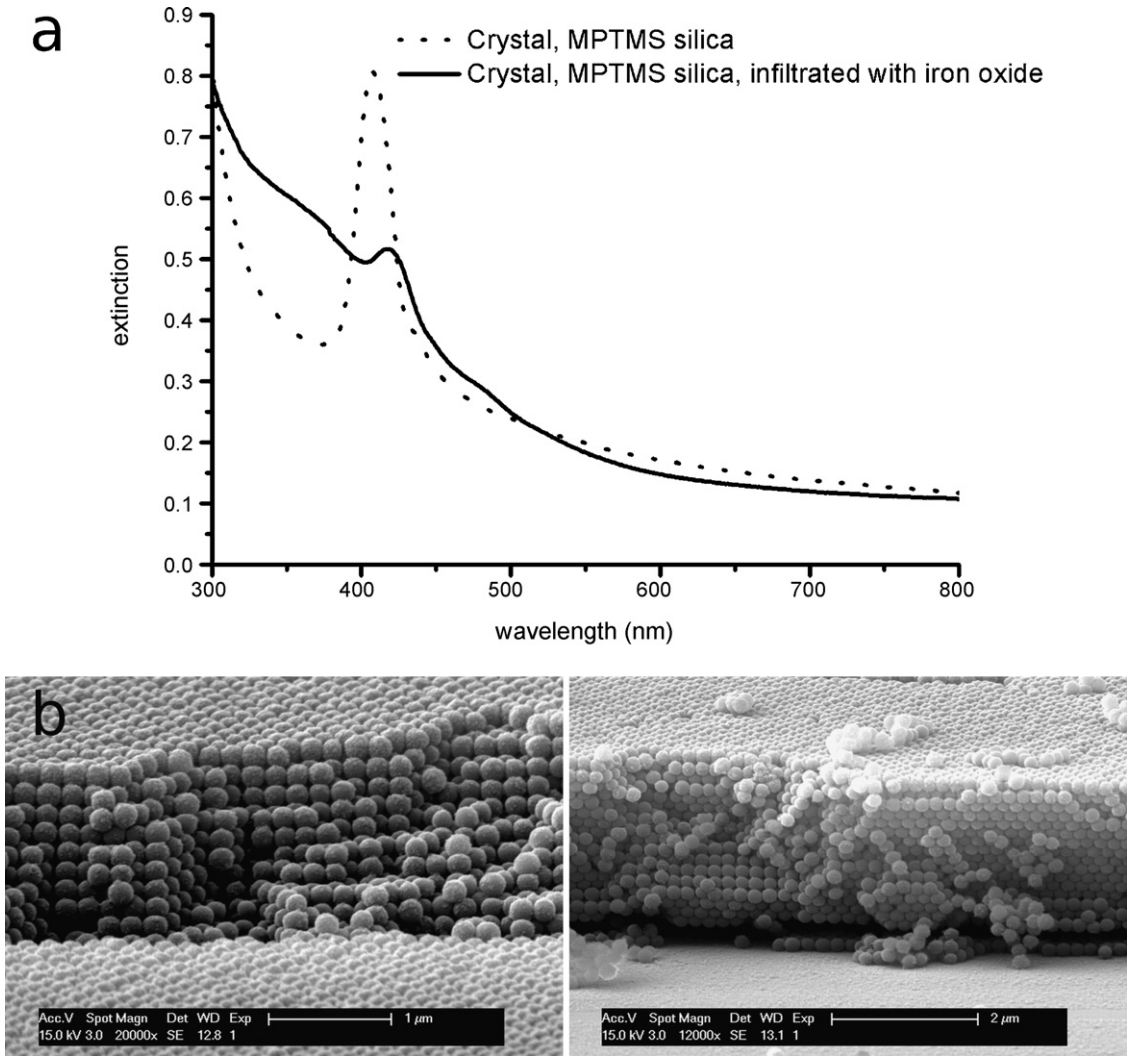

Fig. 4. (a) Extinction spectra recorded in absorbance mode (i.e. the vertical axis is logarithmic). The dotted line shows the spectrum of a crystal made from MPTMS-coated silica colloids, without iron oxide. The solid line shows the spectrum of such a crystal after infiltration with iron oxide particles. (b) SEM images of the crystal that was infiltrated with iron oxide particles after fabrication: long-range ordering is visible.

In all simulations, the colloidal crystals have been represented by monodisperse silica spheres of given size (refractive index of 1.45) arranged along a cubic face centered lattice, i.e. with a packing fraction of 74%. Theoretical calculations were done assuming that the deposition of maghemite was layered, meaning that silica spheres are surrounded by maghemite shells. The filling of the pores (which could be up to 26%) with maghemite (refractive index of 2.42) has been implemented by underfilling the opal with spheres of larger size than the silica ones, but centered at the same positions, thus featuring an underlying interpenetrated maghemite network.

The computational cell, in which the incoming wave propagates along the *z*-direction, has been implemented with periodic boundary conditions in the *x*- and *y*-directions and perfectly matched layers (PMLs) in the *z*-direction. The resolution of the grid has been refined such that the convergence of the results was insured.

4. Results and discussion

Fig. 2a shows a TEM image of the iron oxide particles. The polydispersity of these particles is clearly visible, with an average size of the iron particles determined to be approximately 10 nm. Fig. 2b shows the pair distance distribution function (PDDF) of the iron oxide particles obtained by SAXS. The unsymmetrical shape of the curve suggests that the iron oxide particles are not spherical but more likely to be close to a prolate ellipsoid [34]. D_{max}, defined as the maximum distance within the particle, is about 26.5 nm. From the curve fitting, using a Bayesian weighted inverse Fourier transform [29], a radius of gyration R_G of ~8 nm was calculated for the iron oxide particles. The scattering profile also shows that the particles are highly polydisperse with a mean value around 8 nm. The size of our iron oxide suggests that the particles are superparamagnetic [25]. TEM images (Fig. 2a) allow us to visualize the structure and polydispersity of the iron oxide sample. Note that the TEM images are in excellent agreement with data obtained by SAXS (between 8 and 10 nm).

Because these magnetic particles themselves are too small for photonic applications and due to the lack of transparency, they have to be combined with another material to impart the required structural (monodisperse nanospheres at the optical wavelength scale) and optical properties (transparent). The high polydispersity of the magnetic particles did not allow us to use iron oxide as a core for a shell of silica in order to produce monodisperse core–shell particles, as was described in previous publications [25].

Therefore, we developed an alternative strategy to obtain monodisperse colloids for magnetic photonic crystals, by covalently functionalizing iron oxide particles on top of monodisperse silica spheres. Fig. 3a shows TEM images of iron oxide particles bound to

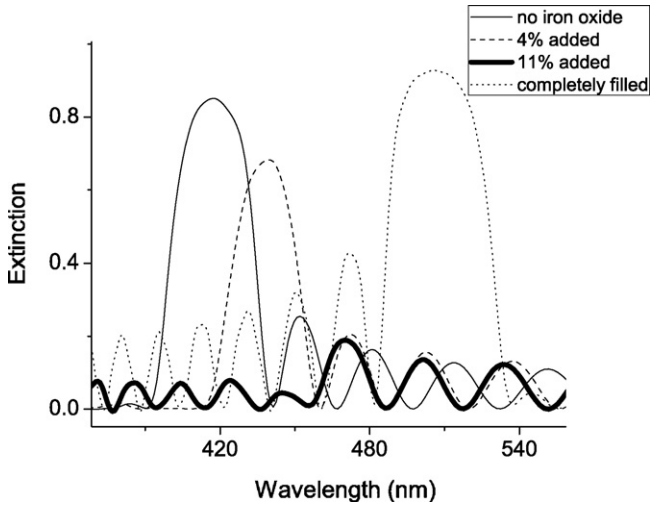

Fig. 5. Simulated transmission spectra showing the effect of increasing amounts of iron oxide in the pores, starting with the silica photonic crystal without iron oxide. A small addition of iron oxide causes a band gap shift without much reduction of the peak. At 11% iron oxide (thick solid line) the band gap almost disappears, to reappear at even longer wavelengths when more iron oxide is introduced until the crystal is completely filled.

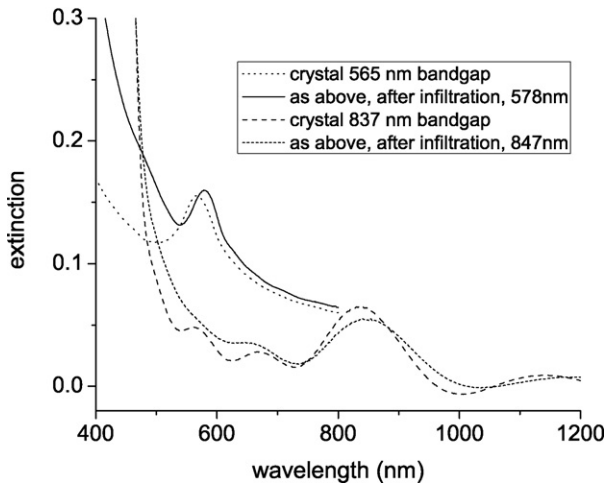

Fig. 6. Photonic crystals with band gaps at 565 and 837 nm, shifting to 578 and 847 nm after infiltration with iron oxide. Only minor amplitude changes are observed, as expected for relatively small amounts of iron oxide compared to the spectra shown in Fig. 4.

the surface of silica particles. These silica/iron oxide coated particles were used in an attempt to fabricate PCs.

Surprisingly these monodisperse hybrid particles cannot produce a highly ordered colloidal crystal as we can see in the SEM images (Fig. 3b). Two factors are probably responsible for this lack of long-range ordering. The most plausible factor is surface roughness which causes steric hindrance between colloids. A second non-negligible factor to be taken into consideration is the presence of magnetic interactions between the magnetic shells. Both of these factors may be responsible for the reduced ordering quality of the crystals made from these hybrid particles, as compared to crystals obtained from bare silica particles.

The lack of ordering is additionally confirmed by optical measurements: transmission spectroscopy does not show a photonic band gap. In fact, the observed spectrum (Fig. 3c) can be explained by a combination of the absorption of the iron oxide and random scattering.

Finally, in order to improve the ordering, colloidal crystals were made by using MPTMS functionalized silica, without iron oxide coating. These crystals show a band gap (Fig. 4a, dotted line) with a peak at 408 nm, in good agreement with the known particle size (200 nm diameter). When these crystals were infiltrated with the iron oxide suspension for 1 h, then rinsed, iron particles remained bound due to the presence of the MPTMS linker. The resulting crystal shows good ordering in SEM imaging (Fig. 4b) and exhibits a band gap in the blue region of the visible spectrum (Fig. 4a, solid line), albeit less pronounced than prior to infiltration, in addition to a strong absorption of light in the UV region due to iron oxide. The shift of the band gap to a slightly longer wavelength can be explained by the introduction of a high refractive index material filling some of the pores in the crystal, thereby increasing the average index of the structure, while the lattice constant remains the same. By using the latter protocol, it is thus possible to fabricate photonic crystals with magnetic functionalities.

The changes in the transmission spectrum observed on infiltration, a shift to longer wavelength and decreased height of the peak, are also confirmed by simulations of a photonic crystal where the voids between the spheres ($n = 1.45$) are gradually filled with a material having a higher index of refraction ($n = 2.42$). These simulation results (Fig. 5) show an increase of the wavelength where the band gap occurs and a decreased peak height as the amount of iron oxide is increased. This explains why we experimentally observe a smaller band gap even though SEM images show good ordering was retained. The simulation also shows the peak becoming bigger again when very large amounts of iron oxide are included, but our infiltration experiments did not reach this point.

Further confirmation of these results was obtained by making photonic crystals from larger silica colloids and infiltrating them with the same iron oxide particles. Such crystals have their band gap at longer wavelengths (see Fig. 6). The iron oxide nanoparticles adsorb on the surface of the silica particles inside the voids of the photonic crystals. It follows that the amount of iron oxide adsorbed is proportional to the surface area, and thus the colloid diameter squared, while the amount of silica is proportional to the volume, or the colloid diameter cubed. Thus, as larger silica colloids are used to prepare the crystal, the relative amount of iron oxide included becomes smaller, and we expect a smaller wavelength shift and

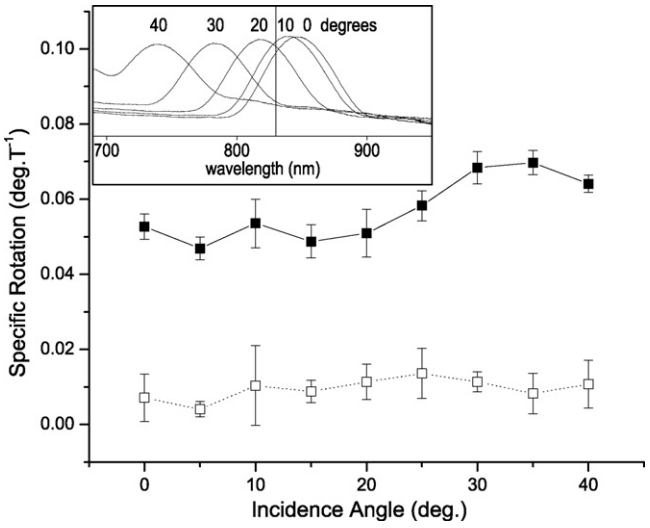

Fig. 7. Experimental setup for Faraday rotation. After passing the polarizer P, the 830 nm laser beam is focused on the sample, mounted on a rotation stage, by a lens L. It is then collimated with a second lens and then traverses an interference bandpass filter IF. Finally, it is directed through the Wollaston prism WP, set at an appropriate angle, at the photodiodes (PDs). The lock-in drives the magnetic coil through the amplifier and detects the signal from the PD in phase and at the same frequency.

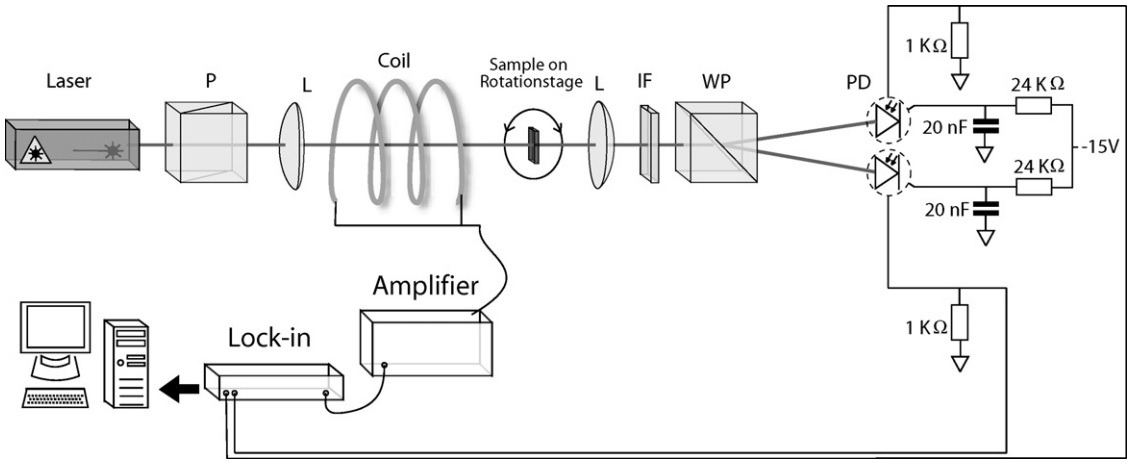

Fig. 8. Results from Faraday rotation measurements at 800 nm on the photonic crystal with band gap at 837 nm (before infiltration with iron oxide particles, open squares) and 847 nm (the same crystal after infiltration, solid squares), with the sample rotated from 0 (perpendicular to the laser beam) to 40°. The inset shows the shift of the band gap to shorter wavelength from 0 to 40° in 10° steps with the laser line at 830 nm indicated by a vertical line.

only a minor effect on the peak height. Transmission spectra confirming this for crystals made using two different colloid sizes are shown in Fig. 6. We also note a pronounced increase in absorption for the infiltrated crystal with band gap at 578 nm, caused by the high optical extinction of the iron oxide at short wavelengths. The much sharper increase of absorption below 500 nm for the crystals with band gap at 837 and 847 nm is however attributed to higher order peaks of the crystal.

In order to demonstrate the effect of magnetic fields on the optical properties of these crystals, Faraday rotation measurements were performed. Faraday rotation data of the photonic crystal before and after infiltration, measured at 830 nm are shown in Fig. 8. The experimental setup is shown in Fig. 7. AC magnetic fields up to 4 G were applied to the sample, ensuring that we stay well below saturation for the magnetic particles. The data show the results of averaging over 4 experiments. The constant background due to the glass substrate was subtracted. After insertion of the magnetic nanoparticles, the specific Faraday rotation of the photonic crystal shows a substantial increase compared to the non-infiltrated crystal. Each sample was measured for incidence angles ranging from 0 to 40° to study the effect of the band gap position for these incomplete band gaps. For these colloidal crystals, which do not exhibit an omnidirectional band gap, the band gap shifts to shorter wavelengths as the sample is rotated away from the perpendicular direction [14]. This means that we can use sample rotation as a way to measure both in and out of the band gap on the same sample. At larger angles, where the band gap is below 830 nm, the Faraday rotation appears to increase even more. Further experimental investigation (wavelength dependence) and theoretical analysis are needed in order to better understand this observation, but a clear positive effect of the presence of the magnetic particles for Faraday rotation in colloidal photonic crystals has been observed.

5. Conclusion

We have developed a successful strategy towards colloidal photonic crystals with combined optical and magnetic properties derived from nanoscale engineering of these two properties at different length scale. Superparamagnetic properties were imparted by the synthesis of small (<20 nm) magnetic maghemite nanoparticles. Optical band gap properties were induced by the convective self-assembly of large (>200 nm) transparent monodisperse silica nanospheres. Insertion of the small magnetic particles after the fabrication of the photonic crystal ensures retention of the photonic band gap upon imparting magnetic functionality. Comparative Faraday rotation measurements confirm the effect of the magnetic particles in a photonic crystal towards enhancing and tuning magnetic interactions in photonic crystals.

Acknowledgments

The authors thank the Research Fund of the KU Leuven for financial support through GOA2006/2 and GOA2006/3, ZWAP 4/07. The Fonds voor Wetenschappelijk Onderzoek Vlaanderen is thanked for a postdoctoral fellowship for R.A.L.V. and for grant G.0458.06. INPAC is thanked for a postdoctoral grant for B.K. All authors warmly acknowledge J. Chen and R. Pitschke (MPI KGF, Golm, Germany) for TEM images, and Thomas Eckert (RWTH Aachen University, Aachen, Germany) for SAXS measurements and useful discussions.

References

[1] A.-H. Lu, E.L. Salabas, F. Schüth, Magnetic nanoparticles: synthesis, protection, functionalization, and application, Angew. Chem. Int. Ed. 46 (2007) 1222.
[2] A.K. Gupta, M. Gupta, Synthesis and surface engineering of iron oxide nanoparticles for biomedical applications, Biomaterials 26 (2005) 3995.
[3] Z. Li, L. Wei, M.Y. Gao, H. Lei, One-pot reaction to synthesize biocompatible magnetite nanoparticles, Adv. Mater. 17 (2005) 1001.
[4] T. Hyeon, Chemical synthesis of magnetic nanoparticles, Chem. Commun. 8 (2003) 927.
[5] A.-H. Lu, W. Schmidt, N. Matoussevitch, H. Bönnermann, B. Spliethoff, B. Tesche, E. Bill, W. Kiefer, F. Schüth, Nanoengineering of a magnetically separable hydrogenation catalyst, Angew. Chem. Int. Ed. 43 (2004) 4303.
[6] S.C. Tsang, V. Caps, I. Paraskevas, D. Chadwick, D. Thompsett, Magnetically separable, carbon-supported nanocatalysts for the manufacture of fine chemicals, Angew. Chem. Int. Ed. 43 (2004) 5645.
[7] S. Mornet, S. Vasseur, F. Grasset, P. Verveka, G. Goglio, A. Demourgues, J. Portier, E. Pollert, E. Duguet, Magnetic nanoparticle design for medical applications, Prog. Solid State Chem. 34 (2006) 237.
[8] H. Schomig, S. Halm, G. Bacher, A. Forchel, A.A. Maksimov, P.S. Dorozhkin, V.D. Kulakovskii, M. Dobrowolska, J.K. Furdyna, Nanooptics on single magnetic semiconductor quantum dots, OSA Trends in Optics and Photonics (TOPS) vol. 89, Quantum Electronics and Laser Science (QELS), Technical Digest, Postconference Edition (Optical Society of America, Washington, DC, 2003) pp. QThe5.
[9] E.M. Claesson, Magnetic core–shell silica particles, Doctoral Thesis, Utrecht University, 2007, ISBN 978-90-393-4559-7.
[10] E.M. Claesson, A.P. Philipse, Monodisperse magnetizable composite silica spheres with tunable dipolar interactions, Langmuir 21 (2005) 9412.
[11] V. Salgueiriño-Maceira, M.A. Correa-Duarte, M. Spasova, L.M. Liz-Marzán, M. Farle, Composite silica spheres with magnetic and luminescent functionalities, Adv. Funct. Mater. 16 (2006) 1266.
[12] E. Yablonovitch, Inhibited spontaneous emission in solid-state physics and electronics, Phys. Rev. Lett. 58 (1987) 2059.
[13] P. Jiang, J.F. Bertone, K.S. Hwang, V.L. Colvin, Single-crystal colloidal multilayers of controlled thickness, Chem. Mater. 11 (1999) 2132.
[14] K. Wostyn, Y.X. Zhao, B. Yee, K. Clays, A. Persoons, G. de Schaetzen, L. Hellemans, Optical properties and orientation of arrays of polystyrene spheres deposited using convective self-assembly, J. Chem. Phys. 118 (2003) 10752.

[15] M. Szekeres, O. Kamalin, R.A. Schoonheydt, K. Wostyn, K. Clays, A. Persoons, I. Dekany, Ordering and optical properties of monolayers and multilayers of silica spheres deposited by the Langmuir–Blodgett method, J. Mater. Chem. 12 (2002) 3268.
[16] S. Reculusa, S. Ravaine, Colloidal photonic crystals obtained by the Langmuir–Blodgett technique, Appl. Surf. Sci. 246 (2005) 409.
[17] H. Míguez, F. Meseguer, C. López, Á. Blanco, J.S. Moya, J. Requena, A. Mifsud, V. Fornés, Control of the photonic crystal properties of fcc-packed submicrometer SiO_2 spheres by sintering, Adv. Mater. 10 (1998) 480.
[18] P. Jiang, M.J. McFarland, Large-scale fabrication of wafer-size colloidal crystals, macroporous polymers and nanocomposites by spin-coating, J. Am. Chem. Soc. 126 (2004) 13778.
[19] A. Mihi, M. Ocana, H. Miguez, Oriented colloidal-crystal thin films by spin-coating microspheres dispersed in volatile media, Adv. Mater. 18 (2006) 2244.
[20] I.L. Lyubchanskii, N.N. Dadoenkova, M.I. Lyubchanskii, E.A. Shapovalov, T. Rasing, Magnetic photonic crystals, J. Phys. D: Appl. Phys. 36 (2003) R227.
[21] M. Inoue, R. Fujikawa, A. Baryshev, A. Khanikaev, P.B. Lim, H. Uchida, O. Aktsipetrov, A. Fedyanin, T. Murzina, A. Granovsky, Magnetophotonic crystals, J. Phys. D: Appl. Phys. 39 (2006) R151.
[22] A. Figotin, I. Vitebsky, Nonreciprocal magnetic photonic crystals, Phys. Rev. E 63 (2001) 066609.
[23] R. Biswas, M.M. Sigalas, G. Subramania, K.-M. Ho, Photonic band gaps in colloidal systems, Phys. Rev. B 57 (1998) 3701.
[24] H.S. Sözüer, J.W. Haus, R. Inguva, Photonic bands—convergence problems with the plane-wave method, Phys. Rev. B 45 (1992) 13962.
[25] K. Baert, W. Libaers, B. Kolaric, R.A.L. Vallee, M. Van der Auweraer, K. Clays, D. Grandjean, M. Di Vece, P. Lievens, Development of magnetic materials for photonic applications, J. Nonlinear Opt. Phys. Mater. 16 (2007) 281.
[26] W. Stöber, A. Fink, E. Bohn, Controlled growth of monodisperse silica spheres in the micron size range, J. Colloid Interface Sci. 26 (1968) 62.
[27] R.A.L. Vallée, K. Baert, B. Kolaric, M. Van der Auweraer, K. Clays, Nonexponential decay of spontaneous emission from an ensemble of molecules in photonic crystals, Phys. Rev. B 76 (2007) 045113.
[28] K. Wostyn, Y.X. Zhao, G. de Schaetzen, L. Hellemans, N. Matsuda, K. Clays, A. Persoons, Insertion of a two-dimensional cavity into a self-assembled colloidal crystal, Langmuir 19 (2003) 4465.
[29] B. Vestergaard, S. Hansen, Application of Bayesian analysis to indirect Fourier transformation in small-angle scattering, J. Appl. Cryst. 39 (2006) 797.
[30] V.K. Valev, J. Wouters, T. Verbiest, Precise measurements of Faraday rotation using ac magnetic fields, Am. J. Phys. 76 (2008) 626.
[31] V.K. Valev, J. Wouters, T. Verbiest, Differential detection for measurements of Faraday rotation by means of ac magnetic fields, Eur. J. Phys. 29 (2008) 1099.
[32] A. Taflove, S.C. Hagness, Computational Electrodynamics: The Finite-Difference Time-Domain Method, third ed., Artech, Norwood, MA, 2005.
[33] A. Farjadpour, D. Roundy, A. Rodriguez, M. Ibanescu, P. Bermel, J.D. Joannopoulos, S.G. Johnson, G. Burr, Improving accuracy by subpixel smoothing in FDTD, Opt. Lett. 31 (2006) 2972.
[34] O. Glatter, in: P. Linder, Th. Zemb (Eds.), Neutrons, X-rays and Light: Scattering Methods Applied to Soft Condensed Matter, North-Holland Delta Series, 2002.